A&A 541, A121 (2012)
DOI: 10.1051/0004-6361/201118738

Astronomy & Astrophysics

The quest for complex molecules in space: laboratory spectroscopy of *n*-butyl cyanide, *n*-C_4H_9CN, in the millimeter wave region and its astronomical search in Sagittarius B2(N)⋆

M. H. Ordu[1], H. S. P. Müller[1,2], A. Walters[3,4], M. Nuñez[3,4], F. Lewen[1], A. Belloche[2], K. M. Menten[2], and S. Schlemmer[1]

[1] I. Physikalisches Institut, Universität zu Köln, Zülpicher Str. 77, 50937 Köln, Germany
e-mail: hspm@ph1.uni-koeln.de
[2] Max-Planck Institut für Radioastronomie, Auf dem Hügel 69, 53121 Bonn, Germany
[3] Université de Toulouse, UPS-OMP, IRAP, Toulouse, France
[4] CNRS, IRAP, 9 Av. colonel Roche, BP 44346, 31028 Toulouse Cedex 4, France

Received 23 December 2011 / Accepted 8 March 2012

ABSTRACT

Context. The saturated *n*-propyl cyanide was recently detected in Sagittarius B2(N). The next largest unbranched alkyl cyanide is *n*-butyl cyanide.
Aims. We provide accurate rest frequency predictions beyond the millimeter wave range to search for this molecule in the Galactic center source Sagittarius B2(N) and facilitate its detection in space.
Methods. We investigated the laboratory rotational spectrum of *n*-butyl cyanide between 75 GHz and 348 GHz. We searched for emission lines produced by the molecule in our sensitive IRAM 30 m molecular line survey of Sagittarius B2(N).
Results. We identified more than one thousand rotational transitions in the laboratory for each of the three conformers for which limited data had been obtained previously in a molecular beam microwave study. The quantum number range was greatly extended to $J \approx 120$ or more and $K_a > 35$, resulting in accurate spectroscopic parameters and accurate rest frequency calculations up to about 500 GHz for strong to moderately weak transitions of the two lower energy conformers. Upper limits to the column densities of $N \leq 3 \times 10^{15}$ cm^{-2} and 8×10^{15} cm^{-2} were derived towards Sagittarius B2(N) for the two lower energy conformers, *anti-anti* and *gauche-anti*, respectively.
Conclusions. Our present data will be helpful for identifying *n*-butyl cyanide at millimeter or longer wavelengths with radio telescope arrays such as ALMA, NOEMA, or EVLA. In particular, its detection in Sagittarius B2(N) with ALMA seems feasible.

Key words. molecular data – methods: laboratory – techniques: spectroscopic – radio lines: ISM – ISM: molecules – ISM: individual objects: Sagittarius B2

1. Introduction

Cyanides account for 20 of the approximately 165 molecules detected in the interstellar medium or in the circumstellar envelopes of late-type stars[1]; not included in this number are isocyanides and other molecules containing the CN moiety. Saturated cyanides are usually found in high-mass star-forming regions, as are other saturated molecules. One part of the Galactic center source Sagittarius (Sgr for short) B2(N) was nicknamed Large Molecule Heimat because of the many and in part rather complex molecules found there, many of them for the first time (Snyder et al. 1994; Menten 2004). Line surveys of the two hot cores Sgr B2(N) and Sgr B2(M) at 3 mm, with selected observations at higher frequencies, have been carried out with the IRAM 30 m telescope to investigate the molecular complexity in these prolific sources. Two cyanides, aminoacetonitrile (NH_2CH_2CN, Belloche et al. 2008), a potential precursor to glycine, and *n*-propyl cyanide along with ethyl formate (*n*-C_3H_7CN and C_2H_5OCHO, Belloche et al. 2009) were detected for the first time in space toward Sgr B2(N) in the course of this study. In addition, ^{13}C isotopologs of vinyl cyanide (C_2H_3CN) were detected for the first time in the interstellar medium, and those of ethyl cyanide (C_2H_5CN) for the first time in this source (Müller et al. 2008); the latter had been identified shortly before in a line survey of Orion KL (Demyk et al. 2007).

With the recent detection of *n*-propyl cyanide, the series of unbranched alkyl cyanides detected in the interstellar medium now contains three members: methyl cyanide, ethyl cyanide, and *n*-propyl cyanide. The chemical models of Belloche et al. (2009) succeeded in reproducing the measured column density ratios with a sequential, piecewise construction of these alkyl cyanides from their constituent functional groups on the grain surfaces, which suggests that this chemical process is their most likely formation route. In addition, these models provide valuable constraints on the possible chemical pathways leading to the formation of complex organic molecules. Detecting the next member in the series of unbranched alkyl cyanides will indeed be a step forward in our understanding of the degree of chemical complexity that can be reached in the interstellar medium.

⋆ Full Table 3 and Tables 4–5 are only available at the CDS via anonymous ftp to cdsarc.u-strasbg.fr (130.79.128.5) or via http://cdsarc.u-strasbg.fr/viz-bin/qcat?J/A+A/541/A121

[1] See e. g. the Molecules in Space page, http://www.astro.uni-koeln.de/cdms/molecules, of the Cologne Database for Molecular Spectroscopy, CDMS.

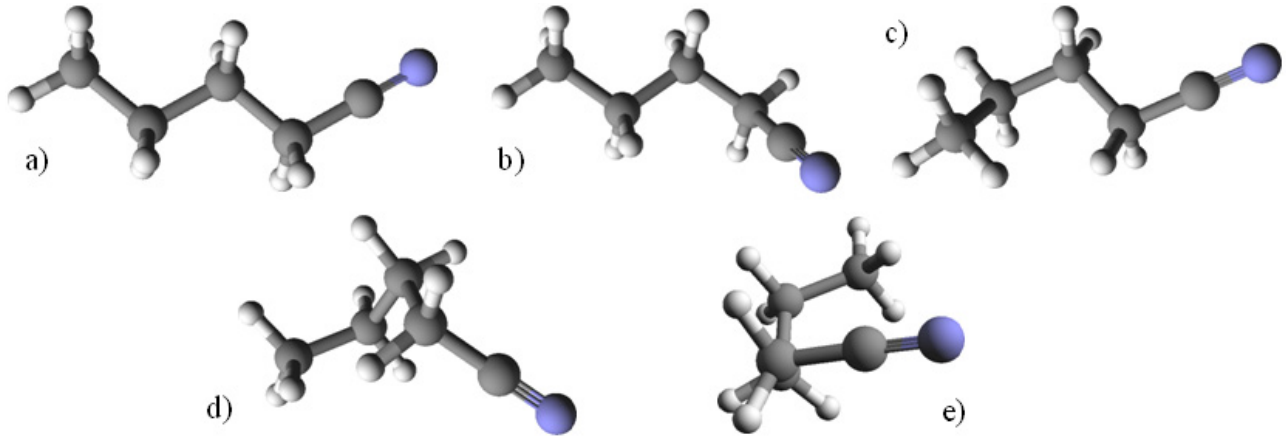

Fig. 1. The conformers of *n*-butyl cyanide. Those investigated in the present work are given in the upper row: **a)** *anti-anti*, **b)** *gauche-anti*, and **c)** *anti-gauche*; the others are in the lower row: **d)** *gauche-gauche*' and **e)** *gauche-gauche*. The ordering is from **a)** being lowest to **e)** being highest in energy. The C and N atoms are indicated by gray and violet "spheres", respectively, and the H atoms by small, light gray "spheres".

A complication of especially high-resolution spectroscopic investigations of *n*-butyl cyanide arises from the different conformations in which the molecule may occur. The *anti-anti* (or *AA*) conformer possesses a planar zig-zag structure of the heavy atoms as demonstrated in Fig. 1. Rotating either the cyano group or the terminal methyl group by about 120° yields the *gauche-anti* (*GA*) and *anti-gauche* (*AG*) conformer, respectively. Since either rotation can be performed clockwise as well as counterclockwise, both conformers are doubly degenerate with respect to the *AA* conformer. Rotating both groups yields two different conformers because they can be rotated to either the same or the opposite side; the former is called *gauche-gauche* (*GG*), while the latter is called *gauche-gauche*' (*GG*'). Both conformers are also doubly degenerate with respect to the *AA* conformer.

Crowder (1989) studied the infrared spectrum of *n*-butyl cyanide in the gas phase. He stated that there are four spectroscopically distinguishable conformers. Among these, *GA* was found to be the most abundant one (46%), *AA* was slightly less abundant (30%), and even *AG* (13%) and a fourth one, presumably rather *GG*' than *GG* (11%), were present. Molecular mechanics[2] calculations yielded *AA* as being the lowest in energy with *GA*, *AG*, and *GG*' being higher by 0.54, 3.68, and 4.31 kJ/mol (or 65, 443, and 519 K), respectively, roughly in accordance with the thermal population of the conformers. Very similar results were obtained for the isoelectronic 1-hexyne.

Bohn et al. (1997) studied the rotational spectrum of *n*-butyl cyanide between 5 GHz and 22 GHz employing molecular beam Fourier transform microwave (MB-FTMW) spectroscopy. Three conformers were identified, *AA*, *GA*, and *AG*. The first two were estimated to be lower in energy than the latter because of the intensities. These findings are in accordance with those from gas-phase infrared spectroscopy mentioned in the previous paragraph. More than 20 rotational transitions were recorded for each conformer with J and K_a extending to 8 and 2, respectively. ^{14}N quadrupole splitting was observed for some transitions, and the diagonal components of the quadrupole tensor were determined.

Quantum chemical investigations into the energetics of the *n*-butyl cyanide conformers have been performed to our knowledge only by Atticks et al. (2002). They carried out Hartree-Fock (HF) and second order Møller-Plesset (MP2) ab-initio calculations for all five conformers of *n*-butyl cyanide. The HF calculations yielded *AA* and *GA* as low-energy conformers with *AG* and *GG*' higher by about 4 kJ/mol (~500 K) and *GG* much higher by more than 8 kJ/mol (~1000 K). This energy ordering is compatible with both spectroscopic studies and is adopted in the present investigation. The higher level MP2 calculations lowered the relative energy of all conformers with a *gauche* orientation of the CN group, but raised the relative energy of *AA*. As a consequence, *AA* and *GG*' were calculated to be essentially isoenergetic. These energies, however, are incompatible with experimental results and are thus discarded.

The previously obtained spectroscopic parameters for three conformers of *n*-butyl cyanide (Bohn et al. 1997) permit reliable predictions up to 40 GHz, partially even 60 GHz. However, already in the 3-mm region, deviations of a few megahertz must be expected. Therefore, we decided to investigate the rotational spectrum of this alkyl cyanide at shorter millimeter wavelengths to facilitate radio-astronomical observations throughout this region. The list of experimental transition frequencies was very greatly increased in the course of the present investigation, as were the frequency and quantum number ranges, permitting strong and medium strong transitions to be predicted accurately into the lower submillimeter-wave region. In addition, we used the data to search for the two lowest energy conformers of *n*-butyl cyanide in our 3 mm line survey of Sgr B2(N).

2. Experimental details

The spectral ranges 75−131 GHz and 200−223 GHz were studied with a new, fully solid-state, source-modulated spectrometer. Detection of the intrinsically weak rotational transitions exhibited by complex molecules required the integration of an absorption cell with an effective path length of 44 m. This double-pass cell comprises three Pyrex tubes of 10 cm diameter and almost equal lengths, and employs both a rooftop mirror, which rotates the polarization by 90 degrees, and a polarizing grid to separate the orthogonal source and detector beams. Millimeter-wave spectrometers with similar double-pass optics have been previously described in the literature, e. g. by Oh & Cohen (1992).

Observations of butyl cyanide absorption features were accomplished by establishing a slow gas flow through the absorption cell. This practice allowed the maintenance of the low and constant pressure (around 6×10^{-3} mbar) required to avoid pressure-broadening over long data acquisition times. Heating

[2] Molecular mechanics is a theoretical model usually based on simplified molecular force fields describing in particular larger molecules.

of the gas inlet valve to about 60 °C was also found to be necessary to avoid sample condensation.

The spectrometer's radiation source consists of a microwave synthesizer covering the 10 to 43.5 GHz range whose output has been amplified, followed by a 3-mm band doubler and a chain of three 2-mm band doublers, respectively. The detector is a waveguide-mounted GaAs Schottky diode, optimally biased with a custom current source constructed at the Universität zu Köln. The detector output is processed by a lock-in amplifier with a time constant of 50 ms; digital averaging of six to eight points typically results in an effective time constant of 300−400 ms.

Additional measurements between 301 and 302 as well as between 342 GHz and 348 GHz employed a phase-locked backward-wave oscillator (BWO) spectrometer, the operating principles of which are described in greater detail in Winnewisser (1995) and Lewen et al. (1998). In the current spectrometer setup, phase locking is achieved by means of a harmonic mixer producing the third harmonic of a frequency-tripled microwave signal. The BWO beam thus stabilized in frequency is directed through a 3.4 m long, 10 cm diameter Pyrex cell and detected with a helium-cooled InSb hot-electron bolometer. Double-passing or larger cell dimensions are not needed here because of the high output power of the BWO (30 mW) and the low noise level of the bolometer. Frequency modulation and referencing are performed as described above.

3. Results

3.1. Laboratory spectroscopy

The rotational spectrum of a large molecule is denser than that of a smaller molecule because the absorbed or emitted flux is distributed over more transitions spanning a larger range of rotational quantum numbers J and K_a, yielding larger partition function values, and possibly over several conformers, increasing partition function values even further. In addition, transitions are observed not only in the ground vibrational state, but also in an increasing number of excited states for increasingly heavier molecules. Some examples illustrate the increase in line density with increasing molecular complexity. The rotational spectra of, e.g., CH_3CN and SO_2 are comparatively sparse such that transitions of $^{13}CH_3^{13}CN$ (Müller et al. 2009) and $SO^{17}O$ (Müller et al. 2000), respectively, can be studied rather extensively by conventional absorption spectroscopy in a sample of natural isotopic composition. And while ^{13}C, and even ^{15}N, isotopologs of vinyl cyanide of natural isotopic composition were studied (Müller et al. 2008; Kisiel et al. 2009), the ^{13}C isotopologs of the only slightly larger (2 H atoms) ethyl cyanide molecule were studied in isotopically enriched samples (Demyk et al. 2007) because the increase in the number of rotational states in each vibrational state as well as the increase in the number of low-lying vibrational states result in a spectrum containing many more lines.

The rotational spectrum of *n*-butyl cyanide was studied in the microwave region initially by absorption spectroscopy by Bohn et al. (1997), but their spectrum turned out to be too dense to perform an in-depth analysis. These authors hence used MB-FTMW, which is a very good alternative way of studying the rotational spectrum of a large complex molecule, in particular for initial assignments, because low rotational temperatures, as low as 1 K, permit only a very small number of rotational levels to be populated compared to room temperature. Bohn et al. (1997) identified more than 20 transitions each between 5 GHz and 22 GHz for the *AA*, *GA*, and *AG* conformers with quantum numbers J and K_a up to 8 and 2, respectively. All three conformers are asymmetric tops where Ray's asymmetry parameter $\kappa = (2B - A - C)/(A - C)$ is close to the prolate limit of −1. The values for the *AA*, *GA*, and *AG* conformers are −0.9898, −0.9229, and −0.9866, respectively. The dipole moment components for each conformer were estimated from that of CH_3CN by rotating the latter molecule such that the CN bonds are parallel. The authors obtained $\mu_a = 3.4$ D and $\mu_b = 1.9$ D for the *AA* conformer, and $\mu_c = 0$ because of the symmetry. The values for the *GA* and *AG* conformers were $\mu_a = 2.3$ D, $\mu_b = 3.1$ D, and $\mu_c \approx 0$ D and $\mu_a = 3.7$ D, $\mu_b \approx 0$ D, and $\mu_c = 1.2$ D, respectively. The diagonal elements of the ^{14}N quadrupole tensor were estimated equivalently from CH_3CN data.

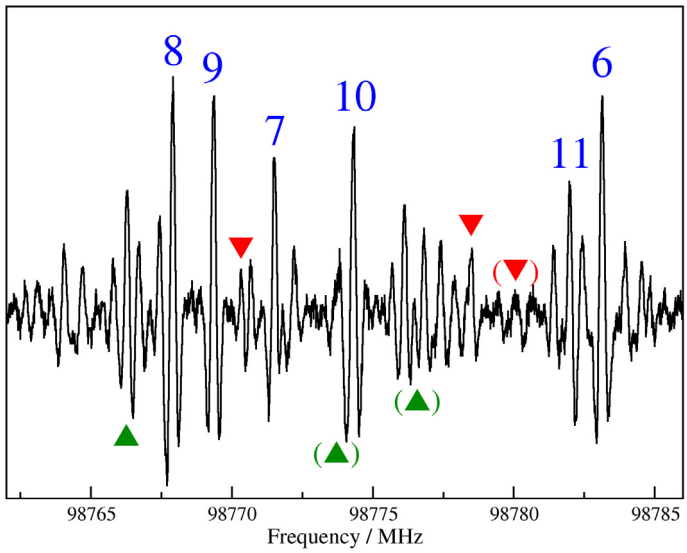

Fig. 2. Section of the millimeter-wave spectrum of *n*-C_4H_9CN displaying features caused by all three conformers investigated in the present analysis. The $K_a' = K_a''$ quantum numbers for the $J = 38-37$ transitions of the *AA* conformer are given in blue (the K_c quantum numbers have been omitted because the asymmetry splitting was not resolved for these transitions). Transitions of the *GA* and *AG* conformers have been marked with triangles pointing upward (green) and downward (red), respectively. Triangles in parentheses are used for overlapped lines or lines with bad line shape. The *AG* lines have $J = 34-33$, and $K_a = 27$, 4, and 28 from left to right; $K_c = J - K_a + 1$ for the $K_a = 4$ line. The *GA* lines belong to *b*-type *Q*-branch transitions with quantum numbers $J_{K_a,K_c} = 40_{9,31}-40_{8,32}$, $69_{7,62}-69_{6,63}$, and $95_{11,84}-95_{10,85}$ from left to right. The lines are presented as second derivatives of a Gaussian line shape because of the $2f$-modulation.

The rotational spectra of the *AA*, *GA*, and *AG* conformers of *n*-butyl cyanide were predicted and fit employing the SPCAT and SPFIT programs by Pickett (1991). The ^{14}N hyperfine structure was not resolved in any of the present measurements because of the rather high quantum numbers and the larger line widths caused by using a free space cell rather than a molecular beam.

Our present measurements were started near 90 GHz. As shown in Fig. 2, the spectrum is very dense, and lines belonging to low-K_a transitions were displaced from the initial predictions by a few megahertz. The large number of lines recorded, the high line density, the presence of lines from three identified conformers, and very many unidentified lines made the analysis time-consuming and delicate particularly in the initial stages before improved predictions were available. Nevertheless, groups of closely spaced lines could be identified unambiguously because the predicted pattern was quite close to the observed one in terms of both frequencies and relative intensities. Improved

Table 1. Spectroscopic parameters[a] (MHz) of three *n*-butyl cyanide conformers.

Parameter	*AA*	*AG*	*GA*
A	15 028.68718(46)	11 887.57688(215)	7635.62496(22)
B	1334.106343(23)	1486.185826(80)	1788.633540(31)
C	1263.857661(22)	1415.762264(76)	1554.221920(33)
$D_K \times 10^3$	214.3780(86)	111.73(207)	52.4008(12)
$D_{JK} \times 10^3$	−7.54309(14)	−2.73331(18)	−9.89990(15)
$D_J \times 10^6$	145.2180(29)	227.0320(80)	861.2105(67)
$d_1 \times 10^6$	−22.0196(20)	−15.7428(83)	−233.3526(72)
$d_2 \times 10^6$	−0.30489(26)	−2.2840(59)	−8.493 0(35)
$H_K \times 10^6$	4.771(32)	2.0[b]	1.452 8(26)
$H_{KJ} \times 10^9$	−53.11(28)	13.05(33)	−351.59(37)
$H_{JK} \times 10^9$	−6.427(11)	−5.849(8)	14.236(19)
$H_J \times 10^{12}$	98.54(13)	137.00(33)	551.63(47)
$h_1 \times 10^{12}$	31.37(15)	−30.46(44)	263.99(156)
$h_2 \times 10^{12}$			24.7(12)
$h_3 \times 10^{12}$			3.00(19)
$L_K \times 10^{12}$			−64.7(15)
$L_{KKJ} \times 10^{12}$	−20.51(15)	−33.57(15)	18.63(31)
$L_{JK} \times 10^{12}$	0.283(13)		−1.257(13)
$L_{JJK} \times 10^{15}$			−9.4(12)
$l_1 \times 10^{15}$			−0.718(82)
$l_2 \times 10^{15}$			−0.327(71)
$P_{KKJ} \times 10^{15}$			−0.353(93)
χ_{aa}	−2.7267(16)	−3.6437(22)	−0.0413(21)
χ_{bb}	0.6753(17)	1.9877(21)	−1.9351(18)
χ_{cc}	2.0514(20)[c]	1.6560(19)[c]	1.9764(16)[c]

Notes. [(a)] Watson's *S* reduction has been used in the representation I^r. Numbers in parentheses are one standard deviations in units of the least significant figures. [(b)] Estimated value, see Sect. 4.1. [(c)] Derived value.

predictions permitted us to assign transitions with higher K_a even if they were isolated. Only transitions were used in the fit for which overlap by unassignable lines or lines from other conformers appeared to be negligible. In the 75.0−130.4 GHz region, *a*-type *R*-branch transitions were used in the fit for all conformers. Many *b*-type transitions were included for the *GA* conformer, as can be expected from the large dipole moment component. In the case of the *AA* conformer, the smaller *b*-dipole moment component initially permitted only $K_a = 1 \longleftrightarrow 0$ transitions to be assigned unambiguously in this frequency region. No *c*-type transitions were assignable unambiguously to the *AG* conformer throughout all frequency regions studied in the course of the present investigation as the dipole moment component is even smaller and the lines of this conformer were weaker because of the much lower abundance than those of the *GA* and *AA* conformers.

The *J* quantum number range was extended by additional measurements between 200.0 GHz and 222.3 GHz. It was straightforward to assign *a*-type transitions for all conformers as well as *b*-type transitions for the *GA* conformer. In addition, a fairly tight $K_a = 8-7$ *Q*-branch was predicted for the *AA* conformer in this frequency region whose relative intensity was quite favorable with respect to the lowest K_a *a*-type *R*-branch transitions. Several transitions of that *Q*-branch could be identified unambiguously and permitted other *b*-type transitions to be identified not only in this frequency region, but also in the 75.0−130.4 GHz region.

Finally, spectral recordings obtained near 300 GHz and 350 GHz were analyzed. Large sections of the $K_a = 13-12$ *Q*-branch of the *AA* conformer appeared to be overlapped negligibly by other features. In addition, some *c*-type transitions of the *AG* conformer appeared to be sufficiently close to the predictions and have about the right intensities, but their number are insufficiently large for us to make unambiguous assignments. Altogether, more than 2200 transitions each have been recorded in the present investigation for the *AA* and *GA* conformers, while almost 1400 transitions have been recorded for the higher energy *AG* conformer. The number of distinct frequencies is smaller by about a factor of two, mainly because of the unresolved asymmetry splitting. The highest *J* values of the transitions included in the fits are around 120 for the *GA* and *AG* conformers and even 136 for the *AA* conformer because of the smaller value of $B + C$. The highest values of K_a are higher than 40 for *GA* and *AG*, and reach a slightly lower value of 38 for the *AA* conformer because of the larger *A* rotational constant.

Among the previous MB-FTMW measurements, the $2_{2,1}-2_{1,2}$ hyperfine components of the *GA* conformer were omitted from the fit because of the rather large and differing residuals. In addition, we excluded from the fit transitions with larger residuals for which no hyperfine splitting was resolved. These were the $8_{08}-7_{07}$ transition of *AA*, the $7_{07}-6_{06}$ transition of *AG*, and the $4_{23}-3_{22}$ transition of *GA*.

Spectroscopic parameters were determined by employing Watson's *S* reduction of the rotational Hamiltonian. The data from the previous MB-FTMW spectroscopic investigation (Bohn et al. 1997) were included in the fit with hyperfine splitting. Parameters were retained in the fit in general if they were determined with significance and if their inclusion contributed to the reduction in the rms error (the reduced χ^2). The resulting spectroscopic parameters are given in Table 1. The transition frequencies with their assignments, uncertainties, and residuals between observed frequency and that calculated from the final set of spectroscopic parameters are available in the supplementary material, as outlined in the appendix, and are also

available in the spectroscopy section[3] of the CDMS (Müller et al. 2001, 2005).

The rms errors of the fits were slightly smaller than 1.0, meaning that the transition frequencies were reproduced on average within the experimental uncertainties. Moreover, partial rms errors for the MB-FTMW data and the present data around 100, 210, and above 300 GHz were mostly between 0.8 and 1.0 and did not exceed 1.1.

3.2. Radioastronomical observations

We used a complete line survey performed in the 3 mm atmospheric window between 80 and 116 GHz toward the hot core region Sgr B2(N). The observations were carried out in January 2004, September 2004, and January 2005 with the IRAM 30 m telescope on Pico Veleta, Spain. Details about the observational setup and the data reduction are given in Belloche et al. (2008). An rms noise level of 15−20 mK on the $T_a^\star$ scale was achieved below 100 GHz, 20−30 mK between 100 GHz and 114.5 GHz, and about 50 mK between 114.5 GHz and 116 GHz.

This survey aims to investigate the molecular complexity of this prolific source and characterize its molecular content. Overall, we detected about 3700 lines above 3σ over the whole 3 mm band. These numbers correspond to an average line density of about 100 features per gigahertz. Given this high line density, the assignment of a line to a given molecule can be trusted only if all lines emitted by this molecule in our frequency coverage are detected with the correct intensity predicted by a model of its excitation *and* if none of the predicted lines are missing in the observed spectrum. It is possible to search for new species once a sufficient number of lines emitted by known molecules have been identified, including vibrationally and torsionally excited states. The XCLASS software[4] is used to model the emission of all known molecules in the local thermodynamical equilibrium approximation (LTE for short), which refers here only to the rotational temperature from which the vibrational or conformational temperatures may differ. More details about this analysis are given in Belloche et al. (2008). About 50 different molecules have been identified in Sgr B2(N) thus far, and for several of them emission or absorption features due to minor isotopologs (about 60) or excited vibrational states (about 50) have also been identified (Belloche et al. in prep.). However, up to as many as 40% of the significant lines remain unassigned, and some of them are rather strong. The article reporting the results of the full survey will be submitted later this year (Belloche et al., in prep.), and the data will become public after acceptance of the article.

We searched for emission features of the *AA* and *GA* conformers of *n*-butyl cyanide in our molecular line survey because these are the two conformers lowest in energy. The *AG* conformer was deemed to be too high in energy to be observable under LTE conditions. Both *AA* and *GA* conformers were assumed to be ground state conformers since the exact energy difference between both conformers is unknown. As a consequence, the derived column density of the higher state conformer, *GA* according to present knowledge, or the upper limit thereof, is likely overestimated. The source size, rotational temperature, line width, and finally the velocity offset from the systemic velocity were assumed to be the same as those for the stronger

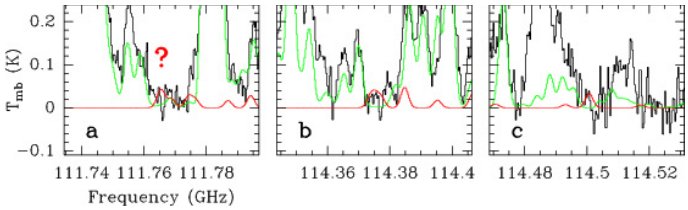

Fig. 3. Sections of the 3 mm line survey of Sgr B2(N) showing the LTE modeling of the astronomical observations. In each panel, the black line represents the observed spectrum and the green line our current model of all firmly assigned species, i. e. without *n*-C_4H_9CN. The red line shows the model corresponding to the parameters listed in Table 2 for the *AA* conformer of *n*-butyl cyanide.

Table 2. Parameters of our best-fit LTE models of alkyl cyanides with upper limits for *n*-butyl cyanide, which was not unambiguously detected.

Molecule[a]	Size[b] (″)	T_{rot}[c] (K)	N[d] (cm^{-2})	ΔV[e] (km s^{-1})	V_{off}[f] (km s^{-1})
(1)	(2)	(3)	(4)	(5)	(6)
CH_3CN	2.7	200	2.0×10^{18}	6.5	−1.0
	2.7	200	8.0×10^{17}	6.5	9.0
	2.7	200	1.0×10^{17}	8.0	−11.0
C_2H_5CN	3.0	170	1.2×10^{18}	6.5	−1.0
	2.3	170	1.4×10^{18}	6.5	9.0
	1.7	170	9.0×10^{17}	8.0	−11.0
n-C_3H_7CN	3.0	150	1.5×10^{16}	7.0	−1.0
	3.0	150	6.6×10^{15}	7.0	9.0
AA-*n*-C_4H_9CN	3.0	150	$\leq 3.0 \times 10^{15}$	7.0	−1.0
GA-*n*-C_4H_9CN	3.0	150	$\leq 8.0 \times 10^{15}$	7.0	−1.0

Notes. [(a)] Results for CH_3CN, C_2H_5CN, and *n*-C_3H_7CN were taken from Belloche et al. (2009). [(b)] Source diameter (FWHM). [(c)] Temperature. [(d)] Column density or upper limit. [(e)] Linewidth (FWHM). [(f)] Velocity offset with respect to the systemic velocity of Sgr B2(N), V_{lsr} = 64 km s^{-1}.

hot-core component of *n*-propyl cyanide (see Table 2). The parameters of the lighter alkyl cyanides are only slightly different.

The partition function values at 300 K and 150 K for the vibrational ground states of the *AA* conformer of *n*-butyl cyanide were calculated as 174 758.2 and 61 661.6. The corresponding values for the *GA* conformer, 191 118.2 and 67 405.2, were calculated neglecting the conformational degeneracy as well as the non-zero energy of the lowest rotational state of the *GA* conformer. Vibrational contributions to the partition function were also neglected because no information is available on the low-lying vibrational states of *n*-butyl cyanide conformers. These contributions are probably not negligible at 150 K and may be very substantial at 300 K, where the latter is the default temperature for the catalog entries and corresponds roughly to the laboratory conditions, and the former is the probable temperature of *n*-butyl cyanide in Sgr B2(N) (see also Table 2). Additional partition function values will be provided in the CDMS.

Most transitions of both conformers are blended with stronger lines of other known species. However, a few transitions are relatively free of contamination and could in principle permit a detection. These are displayed in Figs. 3 and 4. Two transitions of the *AA* conformer coincide with lines that remain unidentified (Figs. 3b and c), but the prediction for another transition may be inconsistent with the observed spectrum depending on the exact position of the baseline, which is uncertain (Fig. 3a). As far as the *GA* conformer is concerned, two transitions coincide with

[3] http://www.astro.uni-koeln.de/cdms/daten
[4] See http://www.astro.uni-koeln.de/projects/schilke/XCLASS

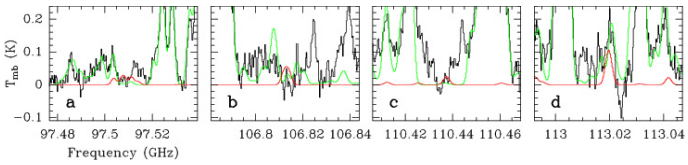

Fig. 4. Same as Fig. 3 but for the slightly higher lying *GA* conformer of *n*-butyl cyanide.

still unidentified lines (Figs. 4a and c), one is partly blended with the weaker velocity component of a vibrationally excited state of C_2H_5CN (Fig. 4b), and one with vibrationally excited dimethyl ether (Fig. 4d).

Overall, the number of potentially detected emission lines of either *n*-butyl cyanide conformer is too small to warrant even a tentative detection. As a result, we consider the models displayed in Figs. 3 and 4 as upper limits to the emission of *n*-butyl cyanide. Therefore, we derive upper limits of 3.0×10^{15} cm^{-2} and 8.0×10^{15} cm^{-2} for the column densities of the *AA* and *GA* conformers of *n*-butyl cyanide, respectively (see Table 2).

4. Discussion

4.1. Laboratory spectroscopy

The present investigations permitted a full set of quartic centrifugal distortion parameters to be determined for the first time for each of the three *n*-butyl cyanide conformers previously characterized by MB-FTMW spectroscopy. In addition, several sextic distortion terms, up to a complete set for *GA*, along with some parameters of even higher order have been obtained with significance. Accurate predictions of the ground-state rotational spectrum are possible for strong to moderately weak transitions throughout the millimeter wave region and well into the submillimeter region for the two lower-energy conformers *AA* and *GA*. In the case of the higher-energy *AG* conformer, which was less well-characterized, predictions of *a*-type transitions should, nevertheless, be reliable up to possibly 500 GHz, but the *c*-type transitions are about as strong or stronger than the *a*-types beyond 300 GHz. However, they are difficult to assign because of the fairly large uncertainties for transitions with K_a higher than 5, and they are still weaker than the transitions of the two more abundant conformers.

Since the two conformers, for which no rotational transitions have been identified thus far, are even higher in energy, it may be difficult to identify them in the recorded spectra. The best prospects should be at lower frequencies because of the fewer as well as narrower lines.

The increase in D_K and the decrease in both D_J and H_J from *GA* to *AG* and then *AA* reflect the increase in *A* and the decrease in $B+C$. A clear trend is also present for the H_K values of the *AA* and *GA* conformers, permitting a value of 2.0 Hz to be estimated for the *AG* conformer. The value may be lower by at least 0.5 Hz or higher by at least 1.0 Hz. No clear trend is discernible for D_{JK} as well as the higher-order diagonal distortion terms. Since *GA* is much farther away from the prolate limit than both *AA* and *AG*, off-diagonal distortion parameters, such as d_1, d_2, etc., play a much bigger role for this conformer than for the other two.

While almost all of the spectroscopic parameters of the three conformers have been firmly determined with small relative uncertainties, some parameters of the *GA* conformer were just barely determined, most notably l_2 and P_{KKJ}. However, the values of both parameters appear to be reasonable. The decline in magnitude from d_1 to d_2 is much more than a factor of 10, while it is about a factor of 10 from h_1 to h_2 and from h_2 to h_3. Hence, it is conceivable that l_1 and l_2 differ by a factor only slightly larger than 2. Similarly, there is a factor of around 10 000 from the magnitude of D_{JK} to that of H_{KJ} to L_{KKJ}, and finally to that of P_{KKJ}. It should be added that the correlation coefficients between l_2 or P_{KKJ} with any of the other spectroscopic parameters are rather small in magnitude, except for those between l_2 and h_2 and between P_{KKJ} and L_{KKJ}, which are fairly large, as expected. As a consequence, omission of l_2 or P_{KKJ} affected only the corresponding lower order parameters, in particular h_2 or L_{KKJ}, respectively. However, these changes were deemed to be too large with respect to their uncertainties, and l_2 and P_{KKJ} were retained in the fit. It is advisable to view their values with caution.

Infrared spectroscopy and low-level theoretical calculations (Crowder 1989; Atticks et al. 2002) predict the *AA* conformer to be the lowest in energy with the *GA* conformer being only slightly higher. The relative energies of the conformers could also be determined from relative intensity measurements in the rotational spectra. In addition to at least reasonable knowledge of the rotational and vibrational contributions to the partition function, one would need to know the dipole moment components accurately. In the case of monocyanides of alkanes or alkenes, the dipole vector is close to being aligned with the CN bond, as in the examples of either vinyl and ethyl cyanide (Kraśnicki & Kisiel 2011) or *iso*-propyl cyanide (Müller et al. 2011), and the total dipole moments are almost the same. The estimates of the dipole moment components for the *n*-butyl cyanide conformers, obtained by rotating the CH_3CN dipole vector such that it is parallel to the CN bond of the respective conformer (Bohn et al. 1997), are hence probably quite good. Small deviations from the alignment with the CN bond, however, as well as uncertainties about the structure may have non-negligible effects on the values of the dipole moment components. Therefore, it is desirable to carry out Stark effect measurements on the *n*-butyl cyanide conformers, which we hope to be able to carry out soon.

We note that higher level (MP2) calculations overestimate the stability of the CN group in the *gauche* conformation compared to the *anti* conformation. Unsurprisingly, a similar situation was encountered for MP2 calculations on *n*-propyl cyanide by Traetteberg et al. (2000), who also describe a gas-phase electron-diffraction study of this molecule carried out at room temperature. The experimentally determined conformational composition, a *gauche* to *anti* ratio of about 3:1, was very similar to the one calculated theoretically. However, these results were recognized to be at variance with results from a microwave study (Wlodarczak et al. 1988) in which relative intensities were measured at room temperature and 233 K. The *anti* conformer was determined to be 1.1 ± 0.3 kJ/mol lower in energy than the *gauche* conformer. A detection of *n*-propyl cyanide in Sgr B2(N) by Belloche et al. (2009) was restricted to lines of the *anti* conformer, since transitions of the *gauche* conformer were too weak at a rotational temperature of 150 K to be detected unambiguously. It was concluded that the *anti* conformer may be even lower in energy than the *gauche* conformer or that the molecules are not in LTE.

The energetics of the *n*-butyl cyanide conformers suggest that a detection in space may only be possible for the *AA* conformer, that the *GA* conformer has some chance of being detected, but that the *AG* conformer, and even more so those not yet characterized by rotational spectroscopy, are likely too high in energy.

4.2. Radioastronomical observations

Since *n*-propyl cyanide has been detected thus far only in the Sgr B2(N) hot core, this source is presently the only viable source to search for *n*-butyl cyanide in space. Column density ratios of 108:80:1 were derived for methyl, ethyl, and *n*-propyl cyanide (Belloche et al. 2009). On the basis of the two heavier molecules, one would expect a column density drop of about two orders of magnitude for *n*-butyl cyanide with respect to *n*-propyl cyanide. However, since methyl and ethyl cyanide have almost equal column densities, the column density of *n*-butyl cyanide may also be quite similar to that of *n*-propyl cyanide. The actual determination of the column density of *n*-butyl cyanide in Sgr B2(N) will thus provide valuable clues to the formation of complex molecules in space.

The upper limits to the column density of the *AA* and *GA* conformers of *n*-butyl cyanide are lower by a factor of 5 and about 2, respectively, than the column density of *n*-propyl cyanide (see Table 2). The much lower, and thus more meaningful, upper limit to the *AA* conformer than the *GA* conformer can be explained by the smaller value of $B + C$ of 2598 MHz versus 3343 MHz and the larger value of $\mu_a \approx 3.4$ D for *AA* versus $\mu_a \approx 2.3$ D and $\mu_b \approx 3.1$ D for *GA* (Bohn et al. 1997, see also Sect. 3.1). Since current knowledge indicates that the *GA* conformer is slightly higher in energy than the *AA* conformer, the column density of the *GA* conformer should be significantly less than twice that of the *AA* conformer at rotational temperatures significantly below room temperature[5]. If an energy difference of 0.54 kJ/mol (65 K) is assumed (Crowder 1989), which is compatible with the abundances derived from IR spectroscopy, the column density ratio between the *AA* and *GA* conformers should be about 1.0:1.2. On the basis of the upper limit of the *AA* conformer, an upper limit to the total *n*-butyl cyanide column density of 6.6×10^{15} cm^{-2} would be derived for the main component of Sgr B2(N). This is more than a factor of two lower than *n*-propyl cyanide. Hence, the possibility of very similar column densities of *n*-propyl cyanide and *n*-butyl cyanide, as mentioned above, may be unlikely. Decreasing the line confusion through interferometric observations should permit us to lower the column-density upper limit of *n*-butyl cyanide or could even lead to its detection. We hope to have observational results from ALMA soon.

Concerning radioastronomical searches for *n*-butyl cyanide more generally, the molecules aminoacetonitrile (Belloche et al. 2008), *n*-propyl cyanide, and ethyl formate (Belloche et al. 2009) were detected most clearly at 3 mm because overlap with frequently stronger lines of lighter or more abundant molecules was not as significant in this frequency region as at either 2 or 1.3 mm. The frequencies are lower than or just reach the Boltzmann peaks of the *a*-type transitions at the derived rotational temperatures of 100 K for aminoacetonitrile (~230 GHz) and ethyl formate (~190 GHz) or 150 K for *n*-propyl cyanide (~200 GHz). With the Boltzmann peak for the *a*-type transitions of the *AA* conformer of *n*-butyl cyanide being at ~150 GHz at 150 K, the molecule is probably most reliably searched for with a single-dish telecope at wavelengths longer than 3 mm. Interferometric observations, e. g. with the Plateau de Bure Interferometer (PdBI, to be upgraded to NOEMA), the Expanded Very Large Array (EVLA), or the Atacama Large Millimeter Array (ALMA), will alleviate the line confusion problem somewhat, which may make searches for the *AA* conformer in space promising at 3 mm or maybe even shorter wavelengths. At any rate, the current laboratory measurements together with the previous ones as well as interpolations should cover all frequencies suitable for the search for *n*-butyl cyanide in space; moreover, extrapolation to higher frequencies is reasonable to some extent.

[5] All *n*-butyl cyanide conformers other than *AA* are conformationally doubly degenerate, whereas *AA* is not degenerate (see Sect. 1).

5. Conclusion

The rotational spectra of three low-lying conformers of *n*-butyl cyanide have been studied extensively in the millimeter and lower submillimeter regions, providing the means to search for this molecule in space. Inspection of our sensitive 3 mm line survey toward Sgr B2(N), carried out with the IRAM 30 m telescope, yielded an upper limit to the column density of the lowest energy *AA* conformer that is considerably lower than the column density found recently for the shorter *n*-propyl cyanide (Belloche et al. 2009). Observations with ALMA, other telescope arrays, or single-dish telescopes at lower frequencies should alleviate the line confusion, leading to a considerable lowering of the upper limit to or the actual detection of the molecule, either of which will provide important clues about the molecular complexity in space. Observational constraints on the column density of *iso*-propyl cyanide, a molecule that has also been studied recently in our laboratory (Müller et al. 2011), will also be interesting as it is the smallest branched cyanide. The detection of this molecule or sufficiently low upper limits to its column densities will provide important information on the importance of branched molecules with respect to their unbranched isomers. Several other complex molecules may also be detectable in this prolific source. It is thus likely that observations of Sgr B2(N) with ALMA around 3 mm will provide deeper insight into astrochemistry.

Acknowledgements. We thank Prof. R. K. Bohn for providing the *n*-butyl cyanide transition frequencies with observed ^{14}N quadrupole splitting. The present investigations have been supported by the Deutsche Forschungsgemeinschaft (DFG) in the framework of the collaborative research grant SFB 956, project B3. H.S.P.M. is very grateful to the Bundesministerium für Bildung und Forschung (BMBF) for financial support through project FKZ 50OF0901 (ICC HIFI *Herschel*) aimed at maintaining the Cologne Database for Molecular Spectroscopy, CDMS. This support has been administered by the Deutsches Zentrum für Luft- und Raumfahrt (DLR). A.W. and M.N. thank the French National Program PCMI (CNRS/INSU) for funding.

Appendix A. Supplementary material

The experimental transition frequencies for the *AA*, *GA*, and *AG* conformers of *n*-butyl cyanide are given as Tables 3, 4 and 5, respectively, in the supplementary material. Only the first and the last 10 lines of Table 3 are shown here; for complete versions of all conformers see the online tables at the CDS. The tables give the rotational quantum numbers J, K_a, and K_c for the upper state followed by those for the lower state. The ^{14}N hyperfine structure was resolved at least in part in the previous measurements (Bohn et al. 1997), so the total spin-rotation quantum number F is given in addition in these cases for the upper and lower states. The observed transition frequency is given in megahertz units with its uncertainty and the residual between observed frequency and that calculated from the final set of spectroscopic parameters. The previous data extend to 22 GHz, and the data from the present investigation start at 75 GHz. Blended transitions are treated by fitting the intensity-averaged frequency, and this weight is also given in the tables. In most cases, the blending is caused by unresolved asymmetry splitting, i.e., the blended transitions agree in terms of their quantum numbers except for K_c

Table 3. Assigned transitions for the *AA* conformer of *n*-butyl cyanide, observed transition frequency (MHz), experimental uncertainty Unc. (MHz), residual O−C between observed frequency and that calculated from the final set of spectroscopic parameters, and weight for blended lines.

J'	K'_a	K'_c	F'	J''	K''_a	K''_c	F''	Frequency	Unc.	O−C	Weight
2	1	2	2	1	1	1	1	5125.020	0.002	−0.00411	
2	1	2	2	1	1	1	2	5125.222	0.002	−0.00453	
2	1	2	3	1	1	1	2	5125.885	0.002	−0.00088	
2	1	2	1	1	1	1	1	5126.047	0.002	−0.00299	
2	1	2	1	1	1	1	0	5126.554	0.002	−0.00219	
2	0	2	2	1	0	1	2	5194.834	0.002	−0.00098	
2	0	2	1	1	0	1	0	5194.972	0.002	−0.00110	
2	0	2	3	1	0	1	2	5195.712	0.002	−0.00048	
2	0	2	1	1	0	1	1	5197.016	0.002	−0.00211	
2	1	1	2	1	1	0	1	5265.520	0.002	−0.00001	
134	15	120		133	15	119		347 645.8987	0.150	0.22104	0.5000
134	15	119		133	15	118		347 645.8987	0.150	0.22104	0.5000
134	17	117		133	17	116		347 670.4872	0.150	0.21437	0.5000
134	17	118		133	17	117		347 670.4872	0.150	0.21437	0.5000
134	18	116		133	18	115		347 700.6380	0.080	−0.04666	0.5000
134	18	117		133	18	116		347 700.6380	0.080	−0.04666	0.5000
134	19	115		133	19	114		347 740.9042	0.080	0.03613	0.5000
134	19	116		133	19	115		347 740.9042	0.080	0.03613	0.5000
134	12	123		133	12	122		347 747.8174	0.080	−0.00769	0.5000
134	12	122		133	12	121		347 747.8174	0.080	−0.00769	0.5000

Notes. This table as well as those of other conformers are available in their entirety at the CDS. A portion is shown here for guidance regarding its form and content.

(prolate paired transitions) or K_a (oblate paired transitions), and both transitions are equal in intensity. Accidental blending of transitions occured occasionally.

References

Atticks, K. A., Bohn, R. K., & Michels, H. H. 2002, Int. J. Quant. Chem., 90, 1440

Belloche, A., Menten, K. M., Comito, C., et al. 2008, A&A, 482, 179

Belloche, A., Garrod, R. T., Müller, H. S. P., et al. 2009, A&A, 499, 215

Bohn, R. K., Pardus, J. L., August, J., et al. 1997, J. Mol. Struct., 413, 293

Crowder, G. A. 1989, J. Mol. Struct. (Theochem), 200, 235

Demyk, K., Mäder, H., Tercero, B., et al. 2007, A&A, 466, 255

Kisiel, Z., Pszczółkowski, L., Drouin, B. J., et al. 2009, J. Mol. Spectrosc., 258, 26

Kraśnicki, A., & Kisiel, Z. 2011, J. Mol. Spectrosc., 270, 83

Lewen, F., Gendriesch, R., Pak, I., et al. 1998, Rev. Sci. Instrum., 69, 32

Menten, K. M. 2004, in The Dense Interstellar Medium in Galaxies, Proc. 4th Cologne-Bonn-Zermatt Symp., Springer Proc. Physics, 91, 69

Müller, H. S. P., Farhoomand, J., Cohen, E. A., et al. 2000, J. Mol. Spectrosc., 201, 1

Müller, H. S. P., Thorwirth, S., Roth, D. A., & Winnewisser, G. 2001, A&A, 370, L49

Müller, H. S. P., Schlöder, F., Stutzki, J., & Winnewisser, G. 2005, J. Mol. Struct, 742, 215

Müller, H. S. P., Belloche, A., Menten, K. M., et al. 2008, J. Mol. Spectrosc., 251, 319

Müller, H. S. P., Drouin, B. J., & Pearson, J. C. 2009, A&A, 506, 1487

Müller, H. S. P., Coutens, A., Walters, A., et al. 2011, J. Mol. Spectrosc., 267, 100

Oh, J. J., & Cohen, E. A. 1992, J. Quant. Spec. Radiat. Transf., 48, 405

Pickett, H. M. 1991, J. Mol. Spectrosc., 148, 371

Snyder, L. E., Kuan, Y.-J., & Miao, Y. 1994, LNP, 439, 187

Traetteberg, M., P. Bakken, P., & Hopf, H. 2000, J. Mol. Struct., 556, 189

Winnewisser, G. 1995, Vib. Spectrosc., 8, 241

Winnewisser, G., Krupnov, A. F., Tretyakov, M. Y., et al. 1994, J. Mol. Spectrosc., 165, 294

Wlodarczak, G., Martinache, L., Demaison, J., et al. 1988, J. Mol. Spectrosc., 127, 178